

Exchange randomness and spin dynamics in the frustrated magnetic Keplerate $\{W_{72}V_{30}\}$

Jürgen Schnack,^{1,*} Ana-Maria Todea,² Achim Müller,² Hiroyuki Nojiri,³
Steven Yeninas,⁴ Yuji Furukawa,⁴ Ruslan Prozorov,⁴ and Marshall Luban⁴

¹*Fakultät für Physik, Universität Bielefeld, Postfach 100131, D-33501 Bielefeld, Germany*

²*Fakultät für Chemie, Universität Bielefeld, Postfach 100131, D-33501 Bielefeld, Germany*

³*Institute for Materials Research, Tohoku University, Katahira 2-1-1, Sendai 980-8577, Japan*

⁴*Ames Laboratory and Department of Physics and Astronomy, Iowa State University, Ames, Iowa 50011, USA*

(Dated: March 22, 2022)

The magnetic properties and spin dynamics of the spin frustrated polyoxometalate $\{W_{72}V_{30}\}$, where 30 V^{4+} ions ($s = 1/2$) occupy the sites of an icosidodecahedron, have been investigated by low temperature magnetization, magnetic susceptibility, proton and vanadium nuclear magnetic resonance, and theoretical studies. The field-dependent magnetization at 0.5 K increases monotonically up to 50 T without any sign of staircase behavior. This low-temperature behavior cannot be explained by a Heisenberg model based on a single value of the nearest-neighbor exchange coupling. We analyze this behavior upon assuming a rather broad distribution of nearest-neighbor exchange interactions. Slow spin dynamics of $\{W_{72}V_{30}\}$ at low temperatures is observed from the magnetic field and temperature dependence of nuclear spin-lattice relaxation rate $1/T_1$ measurements.

PACS numbers: 75.10.Jm, 75.50.Xx, 75.40.Mg

Keywords: Heisenberg model, Frustrated spin system, Numerically exact energy spectrum, NMR

I. INTRODUCTION

Nanometer sized highly symmetric polyoxometalate molecules constitute a fascinating class of molecular materials.^{1–8} The series of Keplerate⁴⁶ clusters $\{Mo_{72}Fe_{30}\}$,^{2,4} $\{Mo_{72}Cr_{30}\}$,⁹ $\{Mo_{72}V_{30}\}$,^{10,11} and $\{W_{72}V_{30}\}$ ¹² is from a magnetism point of view of special interest since in these bodies paramagnetic ions occupy the vertices of a nearly perfect icosidodecahedron – one of the Archimedean solids.

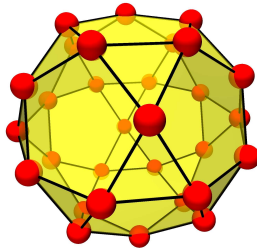


FIG. 1: (Color online) The core structure of the presently investigated Keplerate cluster is an icosidodecahedron. The bullets represent the 30 spin sites and the edges correspond to the 60 exchange interactions between nearest-neighbor spins.

Figure 1 shows the structure of the icosidodecahedron: spin sites are displayed by bullets, edges represent interaction pathways between nearest-neighbor spins, see the Heisenberg model Hamiltonian given in (1). If such interactions are of antiferromagnetic nature, i.e. favor antiparallel alignment in the ground state, a magnetic structure that consists of triangles is said to be frustrated.^{13–15} In this respect the icosidodecahedron be-

longs to the archetypical class of frustrated spin systems made of corner-sharing triangles as does the two-dimensional kagomé lattice antiferromagnet.^{16–21} Compared to other antiferromagnetically coupled spin systems, such as spin rings for instance, these structures possess unusual features generated by the frustration: (1) many low-lying singlet states below the lowest triplet excitation, (2) an extended plateau of the magnetization at one-third of the saturation magnetization when plotted versus field at low temperatures, and (3) a large magnetization jump to saturation, again as function of applied magnetic field.^{19,22–24} The last feature is intimately connected with a huge magnetocaloric effect.^{25,26} It is the hope that valuable insight about the physics of lattices such as the kagomé lattice can be gained by studying the finite-size bodies.

Surprisingly, it turned out that the low-temperature magnetization versus external field B of $\{Mo_{72}Fe_{30}\}$ and $\{Mo_{72}Cr_{30}\}$ deviates substantially from the expectation for a regular icosidodecahedron with a single nearest-neighbor exchange interaction.²⁷ Although the temperature dependence of the weak-field susceptibility could be rather well reproduced by a Heisenberg model with a single exchange constant, the low-temperature magnetization could not. Later investigations revealed a strong dependence at low temperatures T of the differential susceptibility $\partial\mathcal{M}/\partial B$ on T and B .^{27,28} These results were explained in the framework of classical spin dynamics by assuming a distribution of random nearest-neighbor exchange interactions.^{27,28} This means that the exchange interactions between nearest neighbor spins of each molecule in the bulk sample are selected from a random distribution whose mean exchange constant reproduces the high-temperature results. The mere fact that exchange interactions of a real substance might fluctuate

around a mean value might not be surprising. What is indeed surprising is the large spread of values that had to be assumed: the exchange interactions J had to vary from half to twice the mean J (in the non-symmetric distribution).²⁷

In this article we discuss the magnetic properties of a recent member of the family of Keplerates, $\{W_{72}V_{30}\}$, where 30 V^{4+} ions (spins $s = 1/2$) occupy the sites of the icosidodecahedron. In a previous work, the high-temperature ($T > 70$ K) part of the susceptibility data measured at $B = 0.5$ T could be successfully explained using the Quantum Monte Carlo method (QMC) on choosing the antiferromagnetic nearest-neighbor exchange constant $J = -57.5$ K and the spectroscopic splitting factor $g = 1.95$.¹² These numerical values are associated with a Heisenberg Hamiltonian written as

$$\tilde{H} = -2J \sum_{\langle i,j \rangle} \vec{s}_i \cdot \vec{s}_j + g \mu_B B \sum_i s_i^z. \quad (1)$$

Here $\langle i, j \rangle$ indicates a sum over distinct nearest-neighbor pairs and μ_B denotes the Bohr magneton. The QMC method could not be used to establish the magnetic properties of this system below 70 K due to the well-known negative-sign problem for frustrated spin systems.²⁹ Herein lies the important advantage of $\{W_{72}V_{30}\}$: Due to the small spin quantum number, $s = 1/2$, of the individual V^{4+} ions, rather than using classical methods, highly accurate quantum calculations can be performed despite the huge size ($2^{30} = 1,073,741,824$) of the Hilbert space dimension for this system. As shown below, we are able to calculate the relevant thermodynamic observables as functions of both temperature and applied field by means of the Finite-Temperature Lanczos Method (FTLM).^{30,31} In particular, we are able to show that calculations based on (1) on choosing a single value of J do not agree with the measured susceptibility data below 15 K and especially the field-dependence of the low-temperature magnetization. However, we are able to achieve reasonable agreement between theory and experiment upon generalizing (1) so that the numerical value of the exchange constant for any given nearest-neighbor pair is selected using a broad probability distribution constrained so that the mean value equals -57.5 K. Our analysis allows us to estimate the magnitude of the exchange disorder in the compound. As for the other Keplerates, that magnitude is surprisingly large, given the fact that x-ray structure investigations point to a highly symmetric exchange network.

The article is organized as follows. In Sec. II we briefly provide experimental and theoretical details. In Sec. III we provide our experimental results (susceptibility versus T , low temperature magnetization versus B , and NMR measurements) and wherever possible compare with our model calculations. The article closes with a brief summary.

II. EXPERIMENTAL AND THEORETICAL METHODS

Polycrystalline samples of $\{W_{72}V_{30}\} = K_{14}(VO)_2[K_{20} \subset \{(W)W_5O_{21}(SO_4)\}_{12}(VO)_{30}(SO_4)(H_2O)_{63}] \cdot 150 H_2O$ were synthesized using the procedure given in Ref. 12. The temperature dependence of the magnetic susceptibility $\chi = \mathcal{M}/B$ for fixed $B = 0.1$ T was measured at Ames Laboratory in a temperature range of 1.9-300 K using a Quantum Design Magnetic Properties Measurement System. Magnetization measurements were made at the high-field facilities at the Institute for Materials Research (IMR) of Tohoku University. Using pulsed fields, values of the magnetization were achieved for field strengths up to 50 T. Two types of cryostats, a conventional 4He bath type cryostat and a gas-flow type cryostat, were used for the low and high temperature ranges, respectively. Nuclear magnetic resonance (NMR) measurements were carried out at Ames Laboratory on 1H ($I = 1/2, \gamma/(2\pi) = 42.5775$ MHz/T) and ^{51}V ($I = 7/2, \gamma/(2\pi) = 11.193$ MHz/T) by using an in-house phase-coherent spin-echo pulse spectrometer. The NMR spectra were obtained either by Fourier transform of the echo signal or by sweeping B . The NMR echo signal was obtained by means of a Hahn echo sequence with a typical $\pi/2$ pulse length of 1.0 μs . The nuclear spin-lattice relaxation time T_1 was measured by the saturation method with the frequency at the highest peak position of the NMR spectrum.

Our numerical FTLM calculations for the Heisenberg model were performed on a supercomputer. We employed the SGI Altix 4700 as well as the SuperMIG cluster at the German Leibniz Supercomputing Center using openMP parallelization with up to 510 cores.

III. RESULTS AND INTERPRETATION

A. Weak-field susceptibility

Figure 2 (a) shows the temperature dependence of the molar susceptibility χ measured at a field of 0.1 T. The measured data (open red circles, corrected for the effects of diamagnetism and temperature independent paramagnetism) increases monotonically with decreasing T and obeys Curie's law for the lowest T . The latter behavior is due to the presence of the V^{4+} spins of two uncorrelated vanadyl ions, VO^{2+} , per formula unit located between the individual $\{W_{72}V_{30}\}$ molecules.¹² The contribution of these ions, denoted by χ_{imp} , is shown by the solid curve in Fig. 2 (a). Subtracting that contribution from the measured susceptibility yields values of the intrinsic susceptibility, to be denoted by χ_0 , of the $\{W_{72}V_{30}\}$ molecules. This data (solid black circles) shows a broad peak around 20 K and a rapid decrease below approximately 10 K, indicating a singlet ground state for the $\{W_{72}V_{30}\}$ molecule. The data for χ_0 is shown in an expanded scale in Fig. 2 (b). The solid curve corresponds to

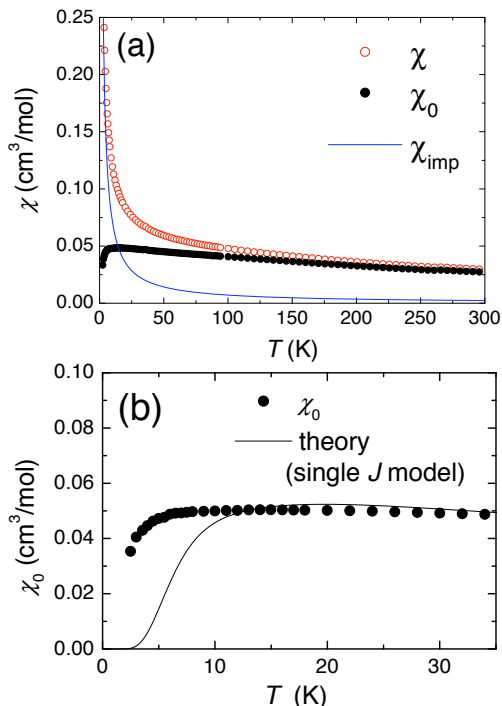


FIG. 2: (Color online) Molar magnetic susceptibility at $B = 0.1$ T as function of temperature: (a) measured data of the crystalline compound (red circles), contribution of two lattice VO^{2+} (solid blue curve), and intrinsic susceptibility χ_0 of the Keplerate cluster $\{\text{W}_{72}\text{V}_{30}\}$ (black circles), compare Ref. 12. (b) intrinsic susceptibility χ_0 (black circles) and theoretical susceptibility using the single- J model (see text).

the results for χ_0 as obtained using the model Hamiltonian of (1) for the above values $J = -57.5$ K and $g = 1.95$ (the “single- J model”). Good agreement between theory and experiment is obtained only for $T > 15$ K. Below that temperature the two data sets depart markedly from each other.

B. Low temperature magnetization

In Fig. 3 the solid blue curve corresponds to our data for the intrinsic magnetization versus external field as obtained by pulsed-field measurements at 0.5 K. The experimental data is corrected for two lattice VO^{2+} . The black dashed-dotted curve is the result obtained for the single- J model. Note the striking staircase behavior of the theoretical curve for this temperature. Surprisingly, the experimental data shows no signs of staircase behavior. This negative result is similar to that for $\{\text{Mo}_{72}\text{Fe}_{30}\}$ and $\{\text{Mo}_{72}\text{Cr}_{30}\}$. The latter systems possess much smaller exchange couplings so one could imagine that the expected steps are more readily washed out due to structural fluctuations or possibly as a result of single-ion anisotropy or Dzyaloshinskii-Moriya interactions.³² However, for the present system the magnetization steps of the theory are

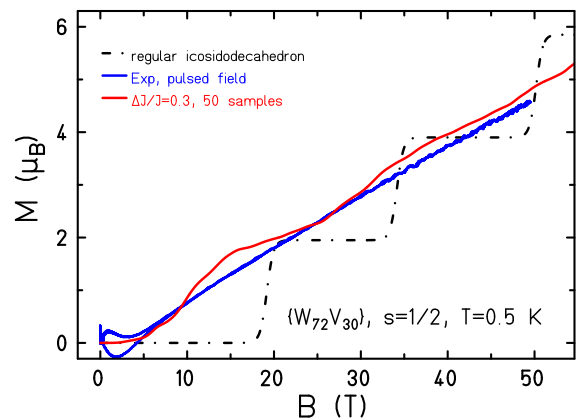


FIG. 3: (Color online) Intrinsic magnetization of the Keplerate anion $\{\text{W}_{72}\text{V}_{30}\}$ as function of applied field for $T = 0.5$ K. Pulsed-field data are given by the blue curve, the theoretical magnetization for the single- J model is shown by the black dashed-dotted curve, and for the multiple- J model with $\Delta J/\bar{J} = 0.3$ by the red curve.

so well separated that one would expect to see at least a hint of them. Moreover, single-ion anisotropy is absent for V^{4+} ions with spin $s = 1/2$.

C. Distribution of nearest-neighbor couplings

In view of the above striking discrepancies between experiment and theory, and in particular the failure of the single- J model at low T values (see also Ref. 27) we assume that this might be due to possible low-temperature structural distortions (as e.g. observed in some kagome lattices^{33–35}), the sensitivity of the exchange interactions on the local environment (highly charged anionic and cationic lattice with many dipolar crystal water molecules that possibly order). It is very important at this point to understand that a symmetric structural distortion that would express itself in just a few distinct exchange interactions would only alter the staircase in a minor way but could not wash it out completely. For this to happen one needs a very large number of different interactions within each and every molecule.

Since the calculations are very computer-intensive we aim for a coarse estimate of the size of the exchange variation. To this end we used a flat distribution with $\bar{J} - \Delta J < J < \bar{J} + \Delta J$ and evaluated the magnetic observables for $\Delta J/\bar{J} = 0.1, 0.2, 0.3, 0.5$, with the mean $\bar{J} = -57.5$ K. Figure 4 shows the magnetization versus field for various choices of ΔJ . As can be deduced already from a small number of samples, step-like behavior persists for $\Delta J/\bar{J} = 0.2$ and below. It turns out that the data for $\Delta J/\bar{J} = 0.3$ comes closest to the experimental data, and that choice is shown as the red curve in Fig. 3. Since we averaged over only 50 samples that curve is still somewhat wiggly but it is sufficiently converged to warrant our conclusions.

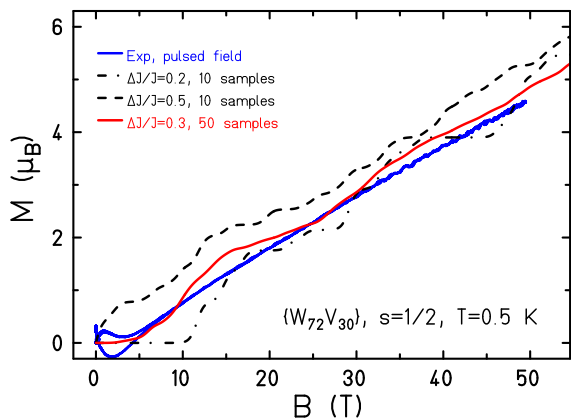


FIG. 4: (Color online) Intrinsic magnetization of the Keplerate anion $\{W_{72}V_{30}\}$ as function of applied field for $T = 0.5$ K. Curves for various exchange variations $\Delta J/\bar{J}$ are compared to the pulsed field data.

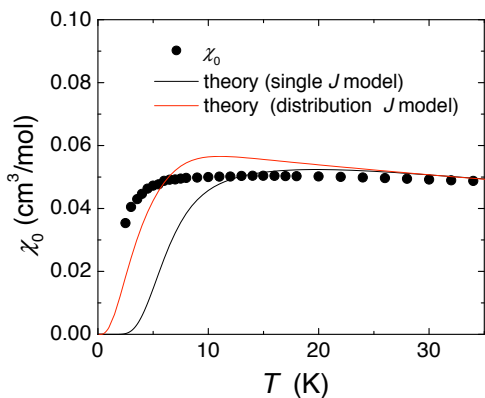


FIG. 5: (Color online) Molar magnetic susceptibility, χ_0 , at $B = 0.1$ T as function of temperature. The curves are the result of our simulations for $\Delta J/\bar{J} = 0.3$ and 0.

Finally, shown in Fig. 5 are the results for the intrinsic susceptibility χ_0 as obtained from our measurements, for the single-J model, as well as for exchange variation with $\Delta J/\bar{J} = 0.3$. We conclude that the introduction of exchange variation yields results that are in reasonably good agreement with our experimental susceptibility data.

D. NMR measurements

1. ^1H -NMR spectrum

^1H -NMR spectra were measured for a magnetic field $B = 2.86$ T as a function of temperature from 1.8 to 150 K. A single NMR line is observed and the line broadens with decreasing temperature as shown in Fig. 6 (a) where the temperature dependence of the line width (full

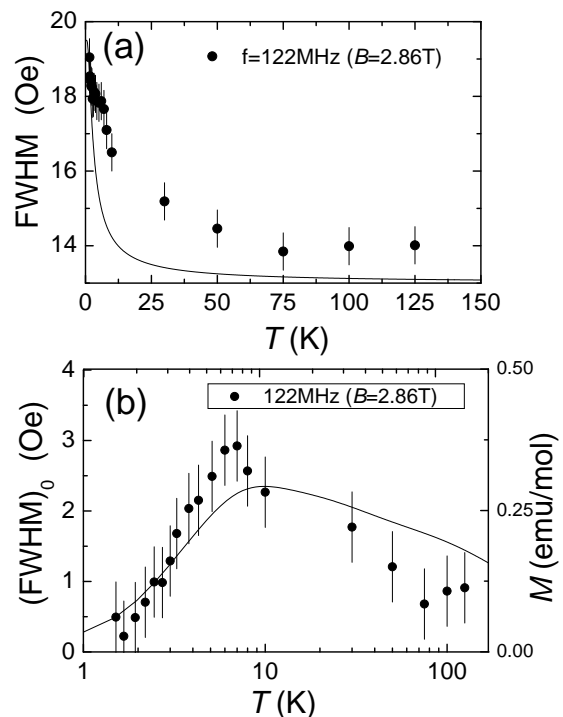


FIG. 6: (a) ^1H -NMR line width (FWHM) at $B = 2.86$ T as a function of temperature. The solid curve shows the fitting result $a + b\mathcal{M}_{\text{imp}}$ (see text). (b) T -dependence of the intrinsic line width, $(\text{FWHM})_0$, given by $c\mathcal{M}_0$. The solid line is the calculated T -dependence of the magnetization with the exchange disorder $\Delta J/\bar{J} = 0.3$ for the same field.

width at half maximum, FWHM) is plotted. The FWHM in $\{W_{72}V_{30}\}$ can be expressed as the sum $a + b\mathcal{M}_{\text{imp}} + c\mathcal{M}_0$. The constant term a originates from nuclear-nuclear dipolar interactions of the order of 10 Oe, and the second and third terms represent the dipolar field contributions produced by the V^{4+} spins of the lattice VO^{2+} ions and the intrinsic magnetic molecule, respectively. The quantities \mathcal{M}_{imp} and \mathcal{M}_0 are the corresponding magnetizations and b and c are parameters related to the average dipolar hyperfine coupling associated with the two sets of V^{4+} spins. In particular \mathcal{M}_{imp} is proportional to the standard expression $\tanh(\mu_B B/k_B T)$ for independent spins $s = 1/2$. The increase of the FWHM at low temperatures is well reproduced by the above expression on choosing $a \sim 13$ Oe and $b \sim 6$ Oe/ μ_B as shown by the solid lines in Fig. 6 (a). By subtracting these contributions from the total FWHM, we obtain the intrinsic line width, to be denoted by $(\text{FWHM})_0$, that is proportional to \mathcal{M}_0 . That data is shown in Fig. 6 (b) and it has a broad peak around 10 K. The solid curve in Fig. 6 (b) corresponds to the theoretical result for \mathcal{M}_0 for exchange disorder $\Delta J/\bar{J} = 0.3$ and for an external magnetic field of $B = 2.86$ T. The experimental data is in reasonable agreement with the theoretical result. In this context one should also keep in mind that the NMR relaxation deviates from a single exponential behavior due

to many inequivalent proton positions of this water rich substance, see also Refs. 36,37.

2. ^{51}V -NMR spectrum

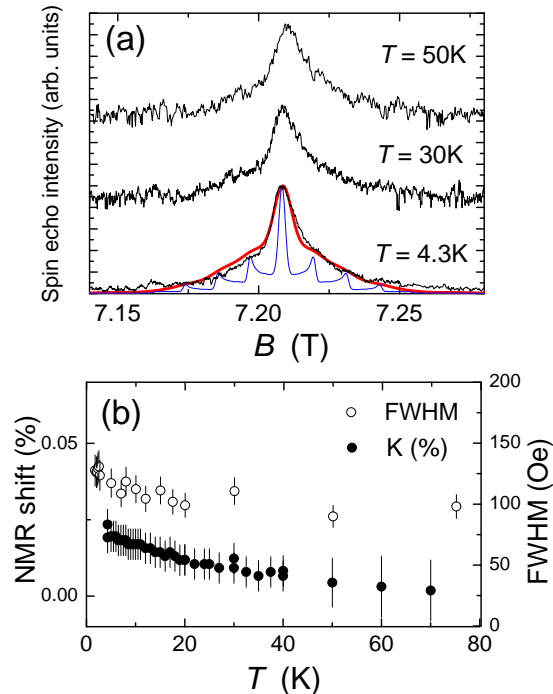


FIG. 7: (Color online) (a) Typical ^{51}V -NMR spectra measured at $f = 80.7$ MHz for various temperatures. The blue curve shows a typical powder-pattern NMR spectrum with $\nu_Q = 0.25$ MHz. The red curve is the simulated NMR spectrum with $\sim 40\%$ distribution of ν_Q . (b) Temperature dependence of ^{51}V NMR shift and line width (FWHM).

Figure 7 (a) shows typical ^{51}V -NMR spectra measured at $f = 80.7$ MHz for various temperatures. The ^{51}V nucleus has nuclear spin $I = 7/2$ so that one expects seven quadrupole-split lines. These spectra can be calculated using a simple nuclear spin Hamiltonian³⁸

$$\tilde{H} = \gamma \hbar \vec{I} \cdot \vec{B}_{\text{eff}} + \frac{h\nu_Q}{6} (3I_z^2 - I(I+1)), \quad (2)$$

where \vec{B}_{eff} is the effective field (the sum of the external field \vec{B} and the hyperfine field \vec{B}_{hf}) at the V^{4+} site, h is Planck's constant, and ν_Q is the nuclear quadrupole frequency. The latter quantity is proportional to the Electric Field Gradient (EFG) at the V^{4+} site (an asymmetric parameter of EFG is assumed to be zero for simplicity). The blue curve in Fig. 7 (a) shows a typical powder-pattern spectrum calculated from the simple Hamiltonian with $\nu_Q = 0.25$ MHz. In order to reproduce the observed spectrum, one needs to introduce a distribution of ν_Q . By taking $\sim 40\%$ distributions ($\Delta\nu_Q \sim 0.1$ MHz),

one can well reproduce the observed spectrum as shown by the red curve in the figure. The wide distribution of ν_Q , which reflects the distribution of the EFG, indicates a high degree of inhomogeneity of the local environments of the vanadium spins, which is mainly due to the large difference between the distances of the two axial V - O bonds, one longer single and one shorter terminal double bond (see crystal structure in Ref. 12).

The temperature dependence of the NMR shift (denoted by K) and FWHM for the ^{51}V NMR spectrum is shown in Fig. 7 (b); both show a very weak temperature dependence. The hyperfine coupling constant can be estimated from the T -dependence of K by comparing with the T -dependence of χ_0 . The resulting value is very small, less than $100 \text{ Oe}/\mu_B$. Usually the hyperfine coupling constant for V^{4+} ions will be dominated by core-polarization, of the order of $-100 \text{ kOe}/\mu_B$,³⁹ which is three orders of magnitude larger than our result. One might attempt to explain the very small value of K by suggesting that the separate contributions to the total hyperfine field from, first, intra-atomic interactions of d electron orbitals and dipolar hyperfine field and, second, the transferred hyperfine field due to other V ions, nearly cancel. We believe, that this is not the case because $1/T_1$ of ^{51}V is almost 50 times smaller than that of ^1H as will be shown in the following section. Since $1/T_1$ is given by a sum of all contributions of the hyperfine fields and each contribution is proportional to the square of the hyperfine coupling constant, it follows that $1/T_1$ of ^{51}V should be larger than that of ^1H even if the total hyperfine field is small due to the cancellation. At present we do not have a clear explanation for the small hyperfine field on V in $\{\text{W}_{72}\text{V}_{30}\}$. It should however be noted that the observed V NMR signal is not coming from non-magnetic V impurities as can be clearly seen in the $1/T_1$ data where ^{51}V - T_1 shows a similar T -dependence with that of ^1H - T_1 .

3. Nuclear spin lattice relaxation rate $1/T_1$

To investigate the dynamical properties of the V^{4+} spins, we have carried out ^1H - T_1 measurements in the temperature range $1.5 - 100$ K. We find that $1/T_1$ is almost independent of temperature above ~ 30 K. Below ~ 30 K, with decreasing temperature, $1/T_1$ starts to increase and then shows a peak around 6 K at $B = 1.17$ T. As the external magnetic field increases, the peak temperature of $1/T_1$ shifts to higher temperatures and at the same time the peak height decreases.

In recent years it has been found,⁴⁰⁻⁴² that in many antiferromagnetic rings and clusters of spins $s > 1/2$ the quantity $1/T_1$ is well approximated by the formula

$$\frac{1}{T_1} = A \chi_0 T \frac{\Gamma}{\Gamma^2 + \omega_L^2}, \quad (3)$$

where the electronic correlation frequency Γ is given by a near-universal power law temperature dependence with an exponent in the range 3.5 ± 0.5 , and A is a fitting

constant independent of both H and T related to the hyperfine field. The form of (3) is due to the fact that the damping of the equilibrium fluctuations of the z -component of the total magnetization, S_z , is monoexponential (Markovian). Specifically this is due to a dynamical decoupling of S_z from the slow degrees of freedom originating from the discreteness of the energy spectrum and the conservation law $[S_z, H_0]$, where H_0 denotes the Heisenberg model Hamiltonian of exchange coupled ion spins.⁴³ It follows from Eq. (3) that the quantity $1/(T_1 T \chi_0)$ has a maximum as a function of T and fixed B when $\Gamma = \omega_L$, and its maximum value is proportional to $1/B$. A quantitative microscopic theory explaining all of these features has been given in Ref. 44 for spins $s > 1/2$ and in particular the numerical value of the power law exponent originates from one-phonon acoustic processes. It is significant that, although $s = 1/2$, our data for $\{W_{72}V_{30}\}$ below 20 K exhibits the very same behavior, and we find $A = 4.7 \times 10^{11}$ rad Hz² mol/(K cm³) and $\Gamma = 6.3 \times 10^5 T^{3.5}$ rad Hz, where T denotes the temperature in units of Kelvins. In $\{W_{72}V_{30}\}$ we find that the paramagnetic fluctuations are dominant for the high-temperature range where the fluctuation frequency is independent of T .

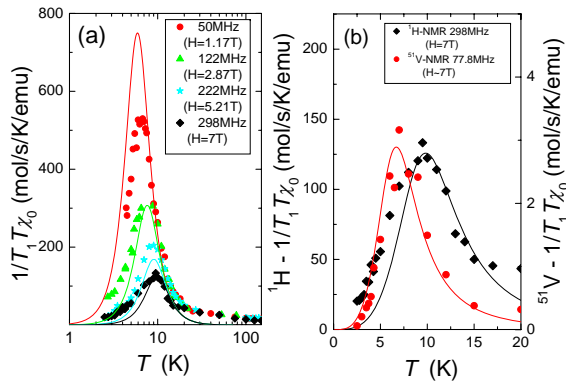


FIG. 8: (Color online) (a) T -dependence of $1/(T_1 T \chi_0)$ for ^1H -NMR. Solid lines are theoretical curves calculated by using (3). (b) T -dependences of $1/(T_1 T \chi_0)$ for ^1H -NMR ($f = 298$ MHz) and ^{51}V -NMR ($f = 77.8$ MHz) at the same magnetic field $B \approx 7$ T (that is, same electron Larmor frequency ω_e).

In general, one expects that (3) should be supplemented by a second Lorentzian, where the nuclear Larmor frequency ω_L is replaced by the electron Larmor frequency ω_e . However, if Γ is of the order of ω_L , the contribution of the second Lorentzian is negligible. To confirm this experimentally, we performed $1/T_1$ measurements on two different nuclei, ^1H and ^{51}V . Values of T_1 for both nuclei were measured at $f = 77.8$ MHz for ^{51}V -NMR and at 298 MHz for ^1H -NMR, respectively, so as to achieve the same value of ω_e , that is the same magnetic field. The two sets of experimental data are shown in Fig. 8 (b) and they are both successfully fitted by (3)

(solid curves). If in (3) one was to include ω_e , the peak position of $1/T_1$ must be observed at the same temperature. These measurements provide a firm confirmation that the fluctuation frequency of V^{4+} spins slow down to the order of MHz.

In antiferromagnetic rings and clusters of spins $s > 1/2$ the peak in $1/(T_1 T \chi_0)$ is usually observed for temperatures of the order of the exchange coupling constant.^{40,43} In Ref. 44 this is explained by the fact that the relaxation mechanism when $s > 1/2$ is governed by the quasi-continuum portion of the quadrupolar fluctuation spectrum and not by the lowest excitation lines. By contrast, in $\{W_{72}V_{30}\}$ we find that the peak temperature ($\approx 6 - 10$ K) is an order of magnitude smaller than $\bar{J} = -57.5$ K. We speculate that this difference in behavior could be explained by invoking the modifications of the microscopic theory proposed in Ref. 44 for spins $s = 1/2$, namely by using a dipolar channel or fluctuating Dzyaloshinskii-Moriya interactions. However, this remains to be confirmed by detailed calculations that are outside the scope of the present work.

IV. SUMMARY

We have investigated magnetic properties and spin dynamics of $\{W_{72}V_{30}\}$ magnetic clusters by low temperature magnetization, magnetic susceptibility, proton and vanadium NMR measurements, and theoretical studies. Our most striking experimental finding is that the field-dependent magnetization at 0.5 K, as obtained using a pulsed magnetic field, increases monotonically up to 50 T without showing any sign of staircase behavior. This is contrary to the predictions of any model based on a single value of the nearest-neighbor exchange coupling. Also we find that a “single-J model” fails to describe the temperature dependence of the intrinsic weak-field magnetic susceptibility χ_0 below 15 K, as obtained from a SQUID measurement. However, both sets of experimental observations are reproduced to reasonable accuracy upon introducing a model based on a broad distribution of values of the nearest-neighbor coupling.

Complementing the SQUID and pulsed fields measurements we have also performed detailed ^1H -NMR and ^{51}V -NMR measurements. We find that the temperature dependence of χ_0 as estimated from the proton NMR spectrum is in satisfactory agreement with that obtained from our SQUID measurements. From the ^{51}V -NMR spectra measurements, a high degree of inhomogeneity of the local environment of V ions is suggested by the observation of a wide distribution of quadrupole frequencies. Inhomogeneity of the local environment is also suggested by the temperature dependence of the observed line width and NMR shift of ^{51}V -NMR. T_1 measurements of both ^1H and ^{51}V reveal the existence of slow spin dynamics at low temperatures. In particular, the fluctuation frequency of the interacting system of V^{4+} spins is found to show a power law behavior, of the form $T^{3.5}$ at temper-

atures below 30 K, i.e., the same behavior that has been found for many antiferromagnetic rings and clusters with spins $s > 1/2$.^{41,44}

Acknowledgment

This work was supported by the Deutsche Forschungsgemeinschaft through Research Unit 945. The work at

the Ames Laboratory was supported by the U.S. Department of Energy-Basic Energy Sciences under Contract No. DE-AC02-07CH11358. H. N. acknowledges the support by Grant in Aid for Scientific Research on Priority Areas (No. 13130204) from MEXT, Japan and by Shimazu Science Foundation. Computing time at the Leibniz Computing Center in Garching is gratefully acknowledged. We thank S. Bud'ko and P. C. Canfield for allowing us to use their MPMS system.

-
- * Electronic address: jschnack@uni-bielefeld.de
- ¹ A. Müller, F. Peters, M. Pope, and D. Gatteschi, *Chem. Rev.* **98**, 239 (1998).
 - ² A. Müller, S. Sarkar, S. Q. N. Shah, H. Bögge, M. Schmidtman, S. Sarkar, P. Kögerler, B. Hauptfleisch, A. Trautwein, and V. Schünemann, *Angew. Chem. Int. Ed.* **38**, 3238 (1999).
 - ³ A. Müller, P. Kögerler, and A. Dress, *Coord. Chem. Rev.* **222**, 193 (2001).
 - ⁴ A. Müller, M. Luban, C. Schröder, R. Modler, P. Kögerler, M. Axenovich, J. Schnack, P. C. Canfield, S. Bud'ko, and N. Harrison, *Chem. Phys. Chem.* **2**, 517 (2001).
 - ⁵ A. Müller, *Science* **300**, 749 (2003).
 - ⁶ U. Kortz, A. Müller, J. van Slageren, J. Schnack, N. S. Dalal, and M. Dressel, *Coord. Chem. Rev.* **253**, 2315 (2009).
 - ⁷ P. Kögerler, B. Tsukerblat, and A. Müller, *Dalton Trans.* **39**, 1 (2010).
 - ⁸ A. Furrer and O. Waldmann, *Rev. Mod. Phys.* **85**, 367 (2013).
 - ⁹ A. M. Todea, A. Merca, H. Bögge, J. van Slageren, M. Dressel, L. Engelhardt, M. Luban, T. Glaser, M. Henry, and A. Müller, *Angew. Chem. Int. Ed.* **46**, 6106 (2007).
 - ¹⁰ A. Müller, A. M. Todea, J. van Slageren, M. Dressel, H. Bögge, M. Schmidtman, M. Luban, L. Engelhardt, and M. Rusu, *Angew. Chem., Int. Ed.* **44**, 3857 (2005).
 - ¹¹ B. Botar, P. Kögerler, and C. L. Hill, *Chem. Commun.* pp. 3138–3140 (2005).
 - ¹² A. M. Todea, A. Merca, H. Bögge, T. Glaser, L. Engelhardt, R. Prozorov, M. Luban, and A. Müller, *Chem. Commun.* pp. 3351–3353 (2009).
 - ¹³ A. P. Ramirez, *Annu. Rev. Mater. Sci.* **24**, 453 (1994).
 - ¹⁴ J. Greedan, *J. Mater. Chem.* **11**, 37 (2001).
 - ¹⁵ J. Schnack, *Dalton Trans.* **39**, 4677 (2010).
 - ¹⁶ P. Sindzingre, G. Misguich, C. Lhuillier, B. Bernu, L. Pierce, C. Waldtmann, and H. U. Everts, *Phys. Rev. Lett.* **84**, 2953 (2000).
 - ¹⁷ R. Moessner, *Can. J. Phys.* **79**, 1283 (2001).
 - ¹⁸ J. L. Atwood, *Nat. Mater.* **1**, 91 (2002).
 - ¹⁹ H.-J. Schmidt, J. Richter, and R. Moessner, *J. Phys. A: Math. Gen.* **39**, 10673 (2006).
 - ²⁰ I. Rousochatzakis, A. M. Läuchli, and F. Mila, *Phys. Rev. B* **77**, 094420 (2008).
 - ²¹ R. Moessner, *J. Phys.: Conf. Ser.* **145**, 012001 (2009).
 - ²² J. Schnack, H.-J. Schmidt, J. Richter, and J. Schulenburg, *Eur. Phys. J. B* **24**, 475 (2001).
 - ²³ J. Schulenburg, A. Honecker, J. Schnack, J. Richter, and H.-J. Schmidt, *Phys. Rev. Lett.* **88**, 167207 (2002).
 - ²⁴ C. Schröder, H. Nojiri, J. Schnack, P. Hage, M. Luban, and P. Kögerler, *Phys. Rev. Lett.* **94**, 017205 (2005).
 - ²⁵ M. E. Zhitomirsky, *Phys. Rev. B* **67**, 104421 (2003).
 - ²⁶ J. Schnack, R. Schmidt, and J. Richter, *Phys. Rev. B* **76**, 054413 (2007).
 - ²⁷ C. Schröder, R. Prozorov, P. Kögerler, M. D. Vannette, X. Fang, M. Luban, A. Matsuo, K. Kindo, A. Müller, and A. M. Todea, *Phys. Rev. B* **77**, 224409 (2008).
 - ²⁸ C. Schröder, X. Fang, Y. Furukawa, M. Luban, R. Prozorov, F. Borsa, and K. Kumagai, *J. Phys.: Condens. Matter* **22**, 216007 (2010).
 - ²⁹ P. Henelius and A. W. Sandvik, *Phys. Rev. B* **62**, 1102 (2000).
 - ³⁰ J. Jaklic and P. Prelovsek, *Phys. Rev. B* **49**, 5065 (1994).
 - ³¹ J. Schnack and O. Wendland, *Eur. Phys. J. B* **78**, 535 (2010).
 - ³² M. Hasegawa and H. Shiba, *J. Phys. Soc. Jpn.* **73**, 2543 (2004).
 - ³³ T. Kambe, Y. Nogami, K. Oshima, W. Fujita, and K. Awaga, *J. Phys. Soc. Jpn.* **73**, 796 (2004).
 - ³⁴ S. A. Reisinger, C. C. Tang, S. P. Thompson, F. D. Morrison, and P. Lightfoot, *Chem. Mater.* **23**, 4234 (2011).
 - ³⁵ H. Yoshida, Y. Michiue, E. Takayama-Muromachi, and M. Isobe, *J. Mater. Chem.* **22**, 18793 (2012).
 - ³⁶ J. K. Jung, D. Procissi, R. Vincent, B. J. Suh, F. Borsa, P. Kögerler, C. Schröder, and M. Luban, *J. Appl. Phys.* **91**, 7388 (2002).
 - ³⁷ J. Lago, E. Micotti, M. Corti, A. Lascialfari, A. Bianchi, S. Carretta, P. Santini, D. Procissi, S. H. Baek, P. Kögerler, et al., *Phys. Rev. B* **76**, 064432 (2007).
 - ³⁸ G. C. Carter, L. H. Bennet, and D. K. Kahan, eds., *Metallic Shift in NMR* (Pergamon, New York, 1977).
 - ³⁹ Y. Furukawa, Y. Nishisaka, K. Kumagai, P. Kögerler, and F. Borsa, *Phys. Rev. B* **75**, 220402 (2007).
 - ⁴⁰ S. H. Baek, M. Luban, A. Lascialfari, E. Micotti, Y. Furukawa, F. Borsa, J. van Slageren, and A. Cornia, *Phys. Rev. B* **70**, 134434 (2004).
 - ⁴¹ F. Borsa, Y. Furukawa, and A. Lascialfari, in *Novel NMR and EPR Techniques*, edited by J. Dolinsek and M. Vilfan and S. Zumer (Springer, New York, 2006).
 - ⁴² P. Santini, S. Carretta, E. Livioti, G. Amoretti, P. Carretta, M. Filibian, A. Lascialfari, and E. Micotti, *Phys. Rev. Lett.* **94**, 077203 (2005).
 - ⁴³ I. Rousochatzakis, *Phys. Rev. B* **76**, 214431 (2007).
 - ⁴⁴ I. Rousochatzakis, A. Läuchli, F. Borsa, and M. Luban, *Phys. Rev. B* **79**, 064421 (2009).
 - ⁴⁵ A. Müller, E. Krickemeyer, H. Bögge, M. Schmidtman, and F. Peters, *Angew. Chem. Int. Ed.* **37**, 3359 (1998).
 - ⁴⁶ The term Keplerate was coined to describe molecular structures that contain Platonic and Archimedean solids because of the use of such structures in an early model of the solar system by Johannes Kepler.⁴⁵